

The properties of void galaxies in the EAGLE simulations

Rosas-Guevara, Yetli ¹

¹ Donostia International Physics Center (DIPC)

Abstract

Cosmic voids, which are underdense regions in the cosmic web, are important because they could be used as laboratories to study the effects of the large-scale environment in the formation and evolution of galaxies since they are expected to be less evolved and preserve the memory of the initial Universe. Indeed, it is expected that in cosmic voids, galaxies are assembled primarily by internal processes and then their properties to be different from galaxies residing in denser environments. In this work, I present the findings of exploring systematically the main properties of central galaxies as a function of the void centric distance using the cosmological hydrodynamic simulation EAGLE and combined with the void catalogue. To understand the differences found, we explore the assembly history of galaxies and discern the possible effects of large-scale environment.

1 Introduction

Cosmic voids, which underdense region with diameters between ~ 1 to ~ 100 Mpc h^{-1} in the Universe, are especially important because they could be used as ideal settings to investigate the influence of the large-scale environment on the formation and evolution of galaxies since they are expected to be less evolved and retain the memory of a more primitive Universe [1]. It is anticipated that galaxies inhabiting cosmic voids are primarily assembled by internal processes, and that their features will differ from those inhabiting other environments. Many observational studies employing galaxy surveys have identified differences in some properties between void galaxies and those residing in denser regions [2]. Generally, void galaxies contain less stellar mass [3], are bluer [4] and with later-type morphology [5]. There is no consensus regarding the differences between some properties of void galaxies and those in denser environments with comparable stellar mass. Using a huge sample of galaxies from SDSS-DR7, [6] have found that void galaxies had higher star formation activity than those lying in the shell of the void or a control galaxy sample. In contrast, when only star forming galaxies were considered, they exhibit the same SF activity as shell void galaxies and a control sample with the same stellar mass distributions. Recently, [7] found comparable mean values of the

specific star formation rates (sSFRs) for void and field galaxies when the sample is limited to star-forming galaxies using 20 cosmic voids that are part of the VGS. Furthermore, the authors found that the molecular and atomic gas masses in void galaxies are comparable to those in galaxies in wall and filaments.

In this work, we present the findings of conducting a systematic investigation of the properties of central galaxies as a function of their location on the cosmic web using the largest simulation of the EAGLE project which are part of the findings in [8]. This simulation, although it is relatively small compared to the largest voids observed in the Universe, allows us to have a representative number of galaxies in diverse regions.

2 Simulations, Void catalogue, galaxy catalogue

We use the largest simulation of the EAGLE project¹ [9]. The largest simulation of EAGLE has a comoving volume of $(100 \text{ cMpc})^3$ with a mass resolution of $9.7 \times 10^6 M_\odot$ for dark matter (and $1.81 \times 10^6 M_\odot$ for baryonic) particles and a softening length of 2.66 ckpc ² limited to a maximum physical size of 0.70 pkpc . The simulation adopts the Λ -CDM cosmology from [10] with cosmological parameters: $\Omega_\Lambda = 0.693$, $\Omega_m = 0.307$, $\Omega_b = 0.04825$, $\sigma_8 = 0.8288$, $h = 0.6777$, $n_s = 0.9611$ and $Y = 0.248$.

We employ the void catalogue presented in [11] at $z = 0$ which is an spherical underdensity finder. The voids are characterised by the void radius, r_{void} and their center. We use the void catalogue in which galaxies with a stellar mass $\geq 10^8 M_\odot$ are tracers.

Our study is limited to galaxies in this study with a stellar mass higher than $10^9 M_\odot$ within a 30-pkpc spherical aperture. We determine the distance between the centre of each galaxy, defined as the position of the minimum potential well, and the centre of all voids provided by the void catalogue. We split the selected galaxies into four samples based on their void-centric distance and in terms of the void radius: **Inner void:** galaxies are defined as those whose minimum void-centric distance is between 0 and $0.8r_{\text{void}}$, where r_{void} is the radius of the closest void; **Outer void:** galaxies whose minimum void-centric distance is between $0.8r_{\text{void}}$ and r_{void} ; **Wall:** galaxies are those located between r_{void} and $1.4r_{\text{void}}$ and **Skeleton:** galaxies are those located beyond $1.4r_{\text{void}}$.

In total, we identified 513 inner void galaxies, 588 outer void galaxies, 7723 wall and 4376 skeleton galaxies, of which 492, 528, 4597 and 1783 are centrals, respectively. This results in 7400 central galaxies in total. Notably, each sample contains a different fraction of satellite galaxies, with the skeleton sample having a satellite fraction of 0.63 whereas 0.05 of the void galaxies are satellites. We focus exclusively on the central galaxies in each sample. We also select smaller samples by requesting to match the same stellar mass distribution of outer, wall and skeleton galaxies to the one of the central galaxies in the inner voids. Hence, the resulting subsamples comprise 492 for inner voids, 461 for outer voids, 3082 for walls, and

¹<http://eaglesim.org>
<http://eagle.strw.leidenuniv.nl>

²Throughout the paper, we refer comoving distances by preceding a 'c' in kpc and physical lengths by a 'p' as pkpc.

1208 for skeleton galaxies.

To visually inspect our classification, the left panel of Fig. 1 depicts the dark matter density map of a slice of $100 \times 100 \times 25$ cMpc from the EAGLE simulation. Circles represent our selected galaxies, and colours correspond to different samples. As seen in the figure and by construction, inner void galaxies (blue circles) are found in the less dense regions of the simulation, whereas skeleton galaxies (magenta circles) are found in the highest-density regions. In intermediate density zones, outer void (green circles) and wall galaxies (orange circles) are located.

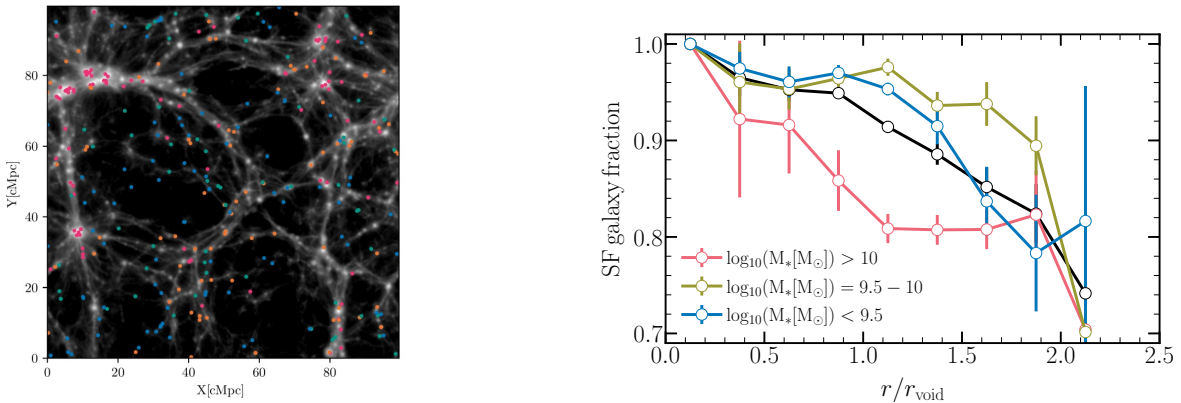


Figure 1: Left panel: A slice of $100 \times 100 \times 25$ cMpc of galaxies in the EAGLE largest simulation at $z = 0$. Blue and green circles, which have same galaxy number density, correspond to inner void and outer void galaxies, respectively. Orange and magenta circles represent wall and skeleton galaxies, respectively. Right panel: The fraction of star-forming galaxies from the parent samples as a function of the void-centric distance and for various stellar mass bins as specified in the legend. Figs. presentend in [8]

3 Results and conclusions

In the right panel of Fig. 1 shows the fraction of star-forming galaxies as a function of void-centric distance and for various stellar mass bins. The error bars correspond to jackknife errors. We define star-forming galaxies as galaxies with a $\text{sSFR} \geq 10^{-11.5} \text{yr}^{-1}$, where $\text{sSFR} = \text{SFR}/M_*$ is the specific star-formation rate in an aperture of 30 pkpc. Star-forming galaxies are slightly more frequent in void galaxies ($> 90\%$) than in exterior regions (80%). When the fraction are estimated for various stellar mass bins, we observe that the decreasing fractions of star-forming galaxies as a function of void-centric distance are maintained. Nevertheless, the fractions fall at different rates.

The top left panel in Fig. 2 shows that galaxies follow the same sequence regardless of their cosmic web location: low stellar mass galaxies are active ($M_* \leq 10^{10} M_\odot$) near the main sequence of star-forming galaxies, whereas massive galaxies have less star-formation activity, with the exception of massive outer void galaxies ($M_* \geq 10^{10} M_\odot$) that appear to have higher

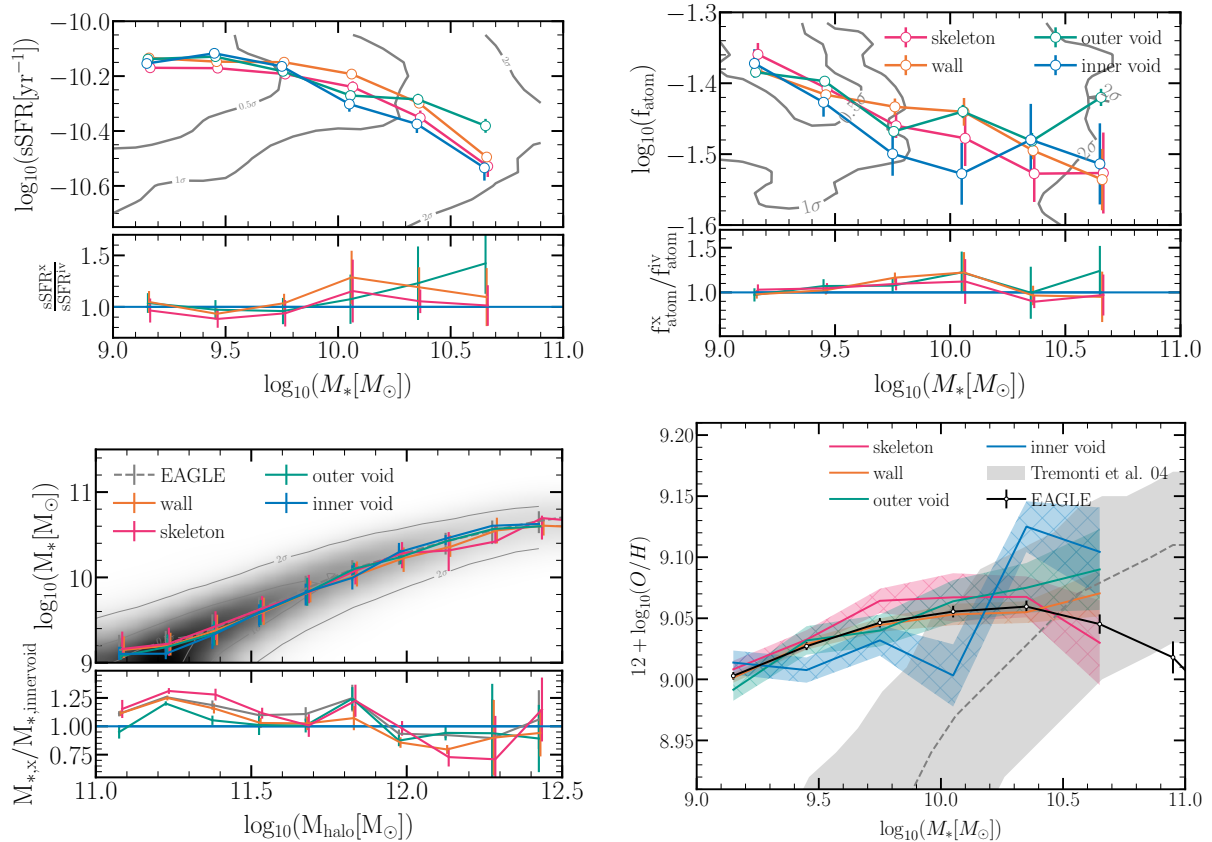


Figure 2: Top panels: The mean specific star formation rate (sSFR, left) and Hydrogen gas fraction (f_{atom} , right) as a function of stellar mass, for each subsample and inner void galaxies. Bottom panels: the halo mass and stellar mass relation (left) and the mean relation between stellar mass and the star-forming gas-phase oxygen abundance (right), contours and density maps represent the distribution of all central galaxies in the simulation. Error bars and shaded regions represent the 20th and 80th percentiles of each sample. Grey dotted line and shaded region are observational estimations from [14]. Figures presented in [8].

star-formation activity. For low mass galaxies ($M_* = 10^{9-9.75} M_\odot$) inner void and outer void galaxies are more active than their wall and skeleton counterparts. For intermediate mass galaxies ($M_* = 10^{9.75-10.25} M_\odot$), we find opposite behaviour depending on if they inhabit the inner/outer void regions or the other regions: inner and outer void galaxies are slightly less SF active than skeleton and wall galaxies. For massive galaxies ($M_* > 10^{10.25} M_\odot$), there is no discernible variation in the star formation activity with the exception of the outer void galaxies, which have a higher star-formation activity.

The top right panel of Fig. 2 shows the average atomic gas fraction, f_{atom} , for each subsample and inner void galaxies. To emphasise the differences in the HI gas fraction between each subsample and the inner void galaxies, the bottom subpanel panel compares the HI gas

fractions of each region to the HI gas fractions of inner void galaxies (see [12] for detailed calculation of HI gas fractions). As can be seen, inner void galaxies with $M_* \geq 10^{9-9.75}M_\odot$ have slightly lower HI gas fractions on average than those in denser regions, although the statistical uncertainties are large. For intermediate stellar masses ($M_* = 10^{9.75-10.25}M_\odot$), it is evident that inner void galaxies have the smallest fractions of HI gas, whereas wall galaxies have the largest fractions compared to other places. Notably, when compared to observations, this is compatible with a recent study by [7] that compared the molecular and atomic gas of control samples of galaxies in filaments and voids using the Void Galaxy Survey (VGS; [15]) and HI data from [13] combined with measurements of CO emission lines. The authors found no significant differences across the samples. However, for these intermediate stellar masses, the atomic gas mass fraction is lower in void galaxies than those in filaments.

The bottom right of Fig. 2 shows the mean relation between the star-forming gas-phase oxygen abundance and the stellar mass for the star-forming galaxies for the subsamples and inner void galaxies. This is the well-known mass-gas phase metallicity relation (MZR). For small galaxies within $M_* = 10^{[9.0,9.5]}M_\odot$, inner void galaxies tend to have higher gas-phase metallicities than those residing in denser regions. For inner void galaxies with $M_* \sim 10^{[9.5,10]}M_\odot$, they have lower gas-phase metallicities than those galaxies residing in denser regions. In particular, the highest difference appears when inner voids are compared with skeleton galaxies. At higher stellar masses ($M_* > 10^{10}M_\odot$), in contrast, the gas-phase metallicity for the inner/outer void galaxies is higher and increases with stellar mass. The gas-phase metallicity for skeleton and wall galaxies flattens with a stellar mass similar to the relation found for the entire central galaxy population.

To understand the shape of the MZR, [16] have studied the evolution of the MZR in EAGLE for different efficiency of AGN feedback and found that the flattening of the MZR in higher stellar mass is due to the action of strong AGN feedback, which possibly generates metal-rich mass-loaded winds. Comparing the MZR from the simulation to the observational relation from [14], shown by the dashed grey band, we do not find an agreement with observational data.

The bottom left panel of Fig. 2 shows the halo mass-stellar mass relation. We find that haloes within voids have a lower stellar mass content than their analogues in denser environments at a fixed halo mass between $10^{11}M_\odot$ and $10^{12}M_\odot$. This is demonstrated in the bottom subpanel of Fig. 2, which compares the median stellar mass of the galaxy subsamples to the median stellar mass in void galaxies (blue line) for a given halo mass. The plot indicates that ratios > 1 appear, with the largest ratio approaching 1.3 in haloes of $M_{\text{halo}} = 10^{11.25}M_\odot$ hosting skeleton galaxies. In general, void galaxies with $M_{\text{halo}} < 10^{12}M_\odot$ have a slightly lower stellar mass than galaxies located in denser environments.

Overall, our results show how large-scale environments could have an effect on the evolution of central galaxies when controlling for stellar mass and that this could have imprinted the properties of the galaxies.

Acknowledgments

The author acknowledges the support of the “Juan de la Cierva Incorporation” fellowship (IJC2019-041131-I), acknowledge support from the Spanish Ministerio de Ciencia e Innovación through project PID2021-124243NB-C21 and support from the European Research Executive Agency HORIZON-MSCA-2021-SE-01 Research and Innovation programme under the Marie Skłodowska-Curie grant agreement number 101086388 (LACEGAL).

References

- [1] van de Weygaert R., Platen E., 2011, *IJMPS*, 1, 41
- [2] Florez, J., Berlind, A. A., Kannappan, S. J., et al. 2021, *ApJ*, 906, 97
- [3] Moorman C. M., Vogeley M. S., Hoyle F., et al., 2015, *ApJ*, 810, 108
- [4] Hoyle F., Vogeley M. S., Pan D., 2012, *MNRAS*, 426, 3041.
- [5] Rojas R. R., Vogeley M. S., Hoyle F., Brinkmann J., 2004, *ApJ*, 617, 50.
- [6] Ricciardelli E., Cava A., Varela J., Quilis V., 2014, *MNRAS*, 445, 4045
- [7] Domínguez-Gómez J., Lisenfeld U., Pérez I., et al., 2022, *A&A*, 658, A124.
- [8] Rosas-Guevara Y., Tissera P., Lagos C. del P., et al., 2022, *MNRAS*, 517, 712
- [9] Schaye, J., Crain, R. A., Bower, R. G., et al. 2015, *MNRAS*, 446, 521
- [10] Planck Collaboration, Ade P. A. R., Aghanim N., Alves M. I. R., Armitage-Caplan C., Arnaud M., Ashdown M., et al., 2014, *A&A*, 571, A1.
- [11] Paillas E., Lagos C. D. P., Padilla N., et al., 2017, *MNRAS*, 470, 4434
- [12] Lagos C. del P., Crain R. A., Schaye J., Furlong M., Frenk C. S., Bower R. G., Schaller M., et al., 2015, *MNRAS*, 452, 3815.
- [13] Kreckel K., Platen E., Aragón-Calvo M. A., et al., *AJ*, 144, 16.
- [14] Tremonti C. A., Heckman T. M., Kauffmann G., et al., 2004, *ApJ*, 613, 898
- [15] Beygu B., Kreckel K., van der Hulst J. M., et al., 2016, *MNRAS*, 458, 394.
- [16] De Rossi M. E., Bower R. G., Font A. S., et al., 2017, *MNRAS*, 472, 3354.